Seventh South African Conference on Computational and Applied Mechanics
SACAM10
Pretoria, 10–13 January 2010

EXPERIMENTAL OBSERVATION OF CAPILLARY INSTABILITIES OF TWO PHASE FLOW IN A MICROFLUIDIC T-JUNCTION

MB Mbanjwa[1,*,†], KJ Land[2*], L Jewell[3,†], EA Moss[4,†] and IMA Gledhill[††]

[*]Mechatronics & Micromanufacturing
CSIR Material Science & Manufacturing, PO Box 395, Pretoria, 0001, RSA,
[1]mmbanjwa@csir.co.za [2]kland@csir.co.za

[†]Faculty of Engineering
University of the Witwatersrand, Private Bag 3, Johannesburg, 2050, RSA,
[3]Linda.Jewell@wits.ac.za, [4]Edward.Moss@wits.ac.za

[††]CSIR Defence, Peace, Safety and Security, PO Box 395, Pretoria, 0001, RSA,
IGledhil@csir.co.za

Keywords: capillary instability, convective instability, microfluidic, T-junction, two-phase flow

Abstract

This paper discusses the experimental observation of capillary instabilities of two-phase flow in a microfluidc T-junction. These instabilities are analogous to the classical Plateau-Rayleigh instabilities. The experiments were carried out with mineral oil and water in a rectangular microchannel of 100 μm width and depth of 75 μm. The interfacial tension of the system was around 3 mN/m after addition of a surfactant in the oil phase. We report on the instabilities observed in three fluid inlet configurations in T-junctions under the same flow parameters. The inlet geometry was found to have limited influence on the behaviour of the flow while the flowrate of the water phase is considered more important.

1 Introduction

The generation of micro- and nanodroplets from immiscible liquid flows in microfluidic systems is finding special interest for use in chemical and biological applications [1-2]. In these microchannel-confined liquid-liquid two-phase flows, capillary instabilities exist as the result of the effect of interfacial tension. Capillary instabilities are analogous to the classical Plateau-Rayleigh instabilities [3-5]. Flow regimes of droplet formation or of stratified flow can be obtained in microfluidic T-junctions depending on the flow conditions of the system. In this paper, we report on the existence of these instabilities under conditions of very low Reynolds numbers for an oil-water flow in T-junction microchannel. Understanding of these instabilities is important for control strategies of two-phase and droplet formation microfluidic systems.

Capillary instabilities in a cylindrical microchannel have, in recent years, received considerable attention from Guillot and co-workers [6-10]. The instabilities in rectangular geometries have been studied in flow focussing [12-13] and a T-junction with symmetrical fluid inlet [6,10-11]. The experiments in the latter work were undertaken in channels made from a hydrophobic material, polydimethyl siloxane (PDMS), but were mounted on a glass substrate. The channels, therefore, were made up of three hydrophobic surfaces and one hydrophilic surface. The hydrophobic surface is wetted by the oil phase and not by the water phase. This results in flow favouring formation of water droplets in the continuous oil flow. We, therefore, refer to oil and water as the continuous phase and the dispersed phase, respectively. The continuous phase does not break into droplets or plugs.

We focus on the nonsymmetric inlet configurations as well as the symmetrical inlet configuration of a microfluidic T-junction made up of only hydrophobic PDMS surfaces. Several studies have focused on the description of the mechanism of droplet breakup in a microfluidic T-junction [14-17], but there is there is little work on the convective instabilities which we have observed in our recent experiments.

2 Scaling Effects and Dimensionless Numbers

The volume forces (gravity and inertia) and surface forces (viscosity and interfacial tension) which interplay in two-phase microfluidic flows can be expressed and evaluated using the basic scaling law and the dimensionless numbers, according to the Birmingham Π-Theorem [18-19]. The scaling law is a concept used in the analysis of a micro-system, whereby the variation of physical quantities is expressed with the length scale of the system, L, while keeping other quantities (time, pressure, temperature, etc) constant [18]. For example:

$$\frac{surface\ forces}{volume\ forces} \propto \frac{L^2}{L^3} = L^{-1} \xrightarrow[L\to 0]{} \infty \qquad (1)$$

Equation (1) implies that the volume forces which are important on a large scale can become insignificant as the length scale decreases, typical of microfluidic flows. Table 1 lists the volume and surface force ratios represented in terms of the important dimensionless numbers, for a characteristic two-phase flow in a microchannel with a hydraulic diameter D_h and average velocity V, where ρ and μ are fluid density and dynamic viscosity, respectively. σ and g represent the interfacial tension and gravity acting on the system.

Table 1: Expression of forces that exist in microfluidic two-phase flows with dimensionless numbers and scaling laws.

Dimensionless number	Equation	Force ratio	Scaling law
Bond number	$Bo = \frac{\rho g D_h^2}{\sigma}$	$\frac{gravitational\ forces}{interfacial\ forces}$	L^2
Capillary number	$Ca = \frac{\mu V}{\sigma}$	$\frac{viscous\ forces}{interfacial\ forces}$	L
Reynolds number	$Re = \frac{\rho V D_h}{\mu}$	$\frac{inertial\ forces}{viscous\ forces}$	L^2
Weber number	$We = \frac{\rho V^2 D_h}{\sigma}$	$\frac{inertial\ forces}{interfacial\ forces}$	L^3

In two phase flow, under miniature conditions, the viscous, inertial and gravitational forces are usually dominated by the interfacial forces, resulting in very low Bond (*Bo*), Capillary (*Ca*) and Weber (*We*) numbers. Also, the viscous effects tend to dominate the inertial forces, favouring flows with small Reynolds (*Re*) numbers. In planar microfluidics, such as ours, gravity effects are neglected and therefore *Bo* is insignificant. The balance between the interfacial and the viscous forces is most significant in determining two-phase flow conditions; hence, *Ca* has been used in the characterisation of these flows. *Ca* calculated for the continuous phase (Ca_c) has been used as a means of describing regimes of droplet formation in a T-junction [14-17]. We, however, characterise the flow based on the Reynolds (Re_c) and Ca_c number for the oil phase (continuous phase; hence subscript) as well as the Reynolds (Re_d), Capillary (Ca_d) and Weber numbers (We_d) for the water phase (dispersed phase; hence subscript).

3 Experimental

3.1 Experimental setup

The experiments were carried out in a rectangular 100μm wide and 75μm deep T-junction microchannel made of transparent PDMS elastomer using soft lithography techniques. The fluids were fed into the microchannel using syringe pumps, which were independently controlled. 10μl/ml (1% v/v) of sorbitan monolaurate (Span 20) surfactant was dissolved in the oil phase, resulting in the interfacial tension of ~ 0.003 N/m. The properties of the fluids are listed in Table 2.

Table 2: Physical properties of the fluids at 25 ^{o}C.

Fluid	Density [kg/m^3]	Viscosity [Pa.s]
Water	997	0.00089
Mineral oil	840	0.0258

The flow was imaged with a digital camera using both standard video mode and high speed mode (1200 frames per second), under a microscope (Figure 1) using a 10x magnification objective lens.

Figure 1: Image of the experimental setup showing two syringe pumps and the microscope.

3.2 Fluid inlet configurations

The different flow configurations were arranged by varying the fluids inlet into the T-junction as illustrated in Figure 2. In the first configuration (Figure 2(a)), which we refer to as the perpendicular configuration, the water is fed into the channel perpendicular to the outlet channel and the oil flow. In the second configuration, the inlets for the fluids is swopped around, whereby, the water is fed into the horizontal channel (Figure 2(b)). The last inlet configuration is the symmetrical (Figure 2(c)). As the name suggests, in this configuration, the oil and the water are fed in the directly opposing direction and exit in the perpendicular channel.

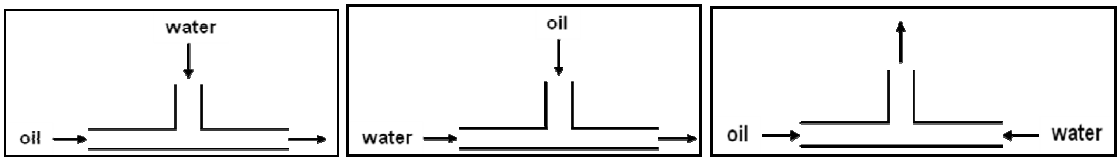

(a) (b) (c)

Figure 2: Flow configurations in a T-junction: (a) perpendicular, (b) horizontal and (c) symmetrical inlets

4 Results and Discussion

4.1 Flow pattern map (perpendicular inlet configuration)

Figure 3 shows the flow pattern map for the perpendicular inlet configuration. The flow patterns were determined by variation of the volumetric flowrates of both the continuous phase (Q_c) and the dispersed (water) phase (Q_d). The flow pattern map was constructed from around 270 flow patterns. The flow patterns are plotted for Q_c values ranging between 0.6

µl/min and 20 µl/min against the flow ratio, Q_d/Q_c, which is directly proportional to Ca_d and Re_d. The Q_c values correspond to Ca_c values of between 0.011 and 0.38.

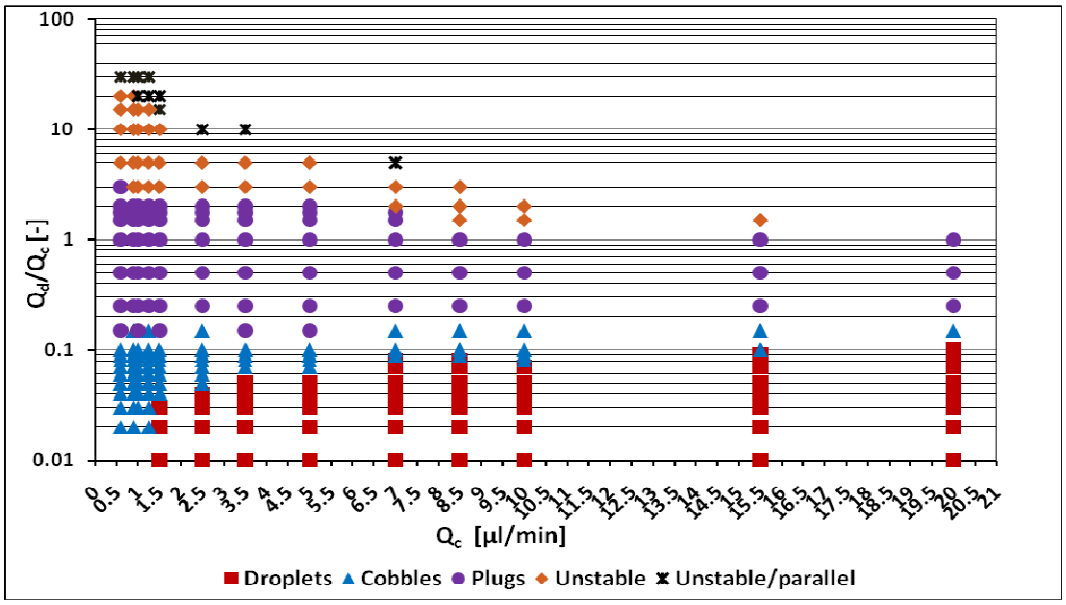

Figure 3: Flow pattern map of T-junction (perpendicular inlet configuration). The abscissa values correspond to Ca_c values between 0.011 and 0.38

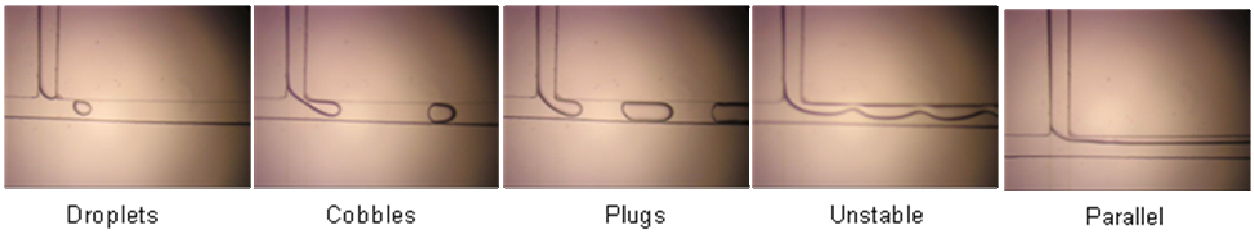

Figure 4: Images of different flow patterns as observed in a T-junction.

The map shows that the breaking up of the water phase into droplets, cobbles and plugs (Figure 4) is dependent on both Q_c and Q_d/Q_c. The map shows that at low to intermediate Q_c values, droplets, cobbles and plugs are dominant at Q_d/Q_c values between 0.01 and 1, above which unstable flow begins to prevail (Figure 4). At higher Q_c values the instabilities can begin occurring in the limit of Q_d/Q_c equal to 1 and below. The inertial effects begin dominating in the water phase, as characterised by increasing We_d. The instabilities begin at the junction and evolve in the channel and are characterised by long wavelengths. The perturbations propagate in the direction of the flow and the water phase does not break into droplets. We refer to this behaviour as the convective instability or unstable stratified flow. In the flow regime between unstable and parallel flows exists a flow regime where the instabilities begin at the junction but are dampened into parallel flow (Figure 5). This is attributed to viscosity effects. The viscosity of the water is about 30 times less than that of oil.

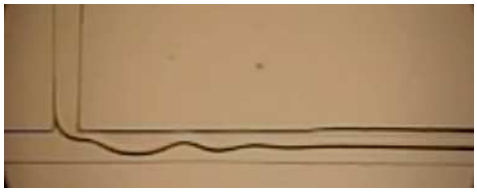

Figure 5: Dampening of convective instability into parallel flow

4.2 Transition between convectively unstable flow and plug breakup

The experiments show there is existence of two or more types of flow regimes and instabilities under the same experimental conditions. There are variations in the time of regimes which depend on the flow conditions. For example, the cycles of convective instability remains for a certain period, after which the flow switches to the regime where break up into droplets, cobbles or plugs occurs (Figure 6). Other flow patterns may also exist e.g. in some cases the stratified parallel flow exists in the transition from plug formation to unstable stratified flow (Figure 6(c)).

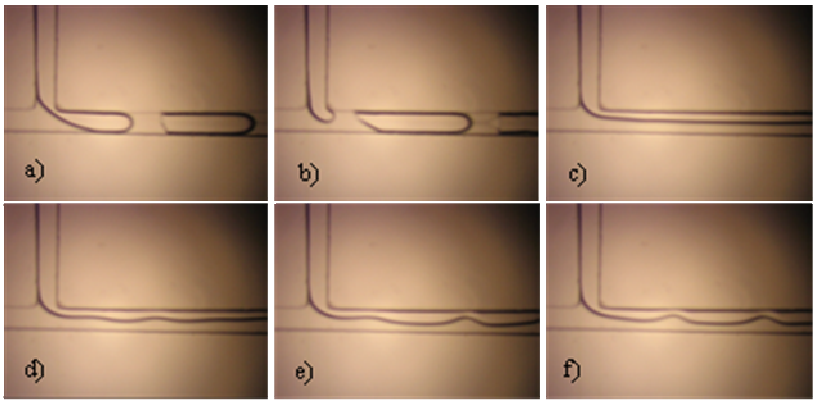

Figure 6: Transition from plugs into unstable stratified flow. The time interval between the snapshots (a-f) is 0.25 seconds.

The plugs get elongated before the flow is switched to a parallel flow and then becomes convectively unstable. The parallel flow does not occur in the transition from unstable stratified flow into the plug formation regime. Figure 7 shows the transition from unstable stratified flow into plug formation. The water phase breaks up into plugs for a certain period before switching back into the unstable stratified flow.

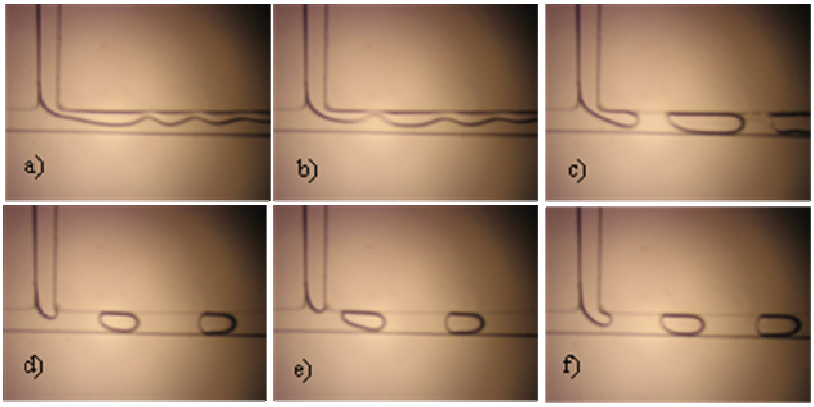

Figure 7: Transition from unstable stratified flow into plug formation. The time interval between the snapshots (a-f) is 0.25 seconds.

4.3 Influence of fluid inlet geometry

The results of instability behaviour under varying fluid inlet geometries are presented in Figures 8-11 and Table 3. The experiments were conducted at varying Q_c and Q_d conditions. In many of the unstable flow cases, the flow was identical except for some conditions in which the symmetrical inlet configuration deviated (see Table 3). In the cases where parallel flow was observed, it was similar in all three geometric configurations.

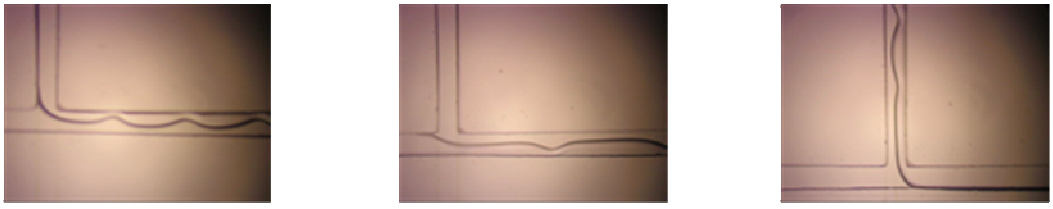

Figure 8: Unstable stratified flow at Qc = 5µl/min, Q = 8, Ca_c = 0.1, Re_c = 0.031, Ca_d = 0.026 Re_d = 8.6, We_d = 0.23 for different flow inlet configurations (a) perpendicular, (b) horizontal and (c) symmetrical. No different cycles of instability were observed under these conditions.

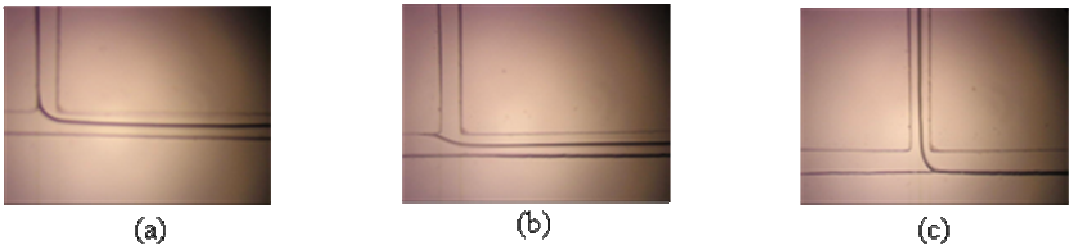

Figure 9: Parallel flow at Qc = 5µl/min, Q =16, Ca_c = 0.1, Re_c = 0.031, Ca_d = 0.053 Re_d = 17.1, We_d = 0.9 for different flow inlet configurations (a) perpendicular, (b) horizontal and (c) symmetrical.

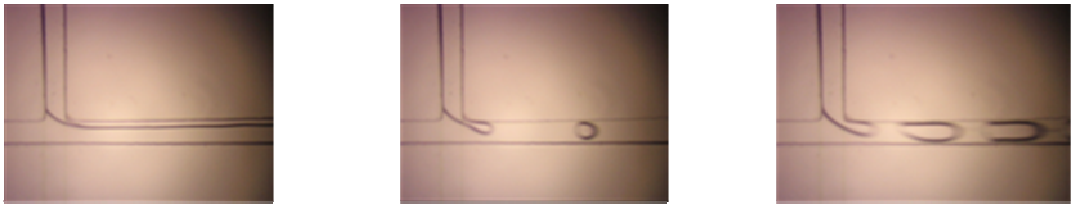

Figure 10: Cycles between (a) stable parallel flow, (b) droplet and (d) plug formation at Qc = 25µl/min, Q =1, Ca_c = 0.48, Re_c = 0.16, Ca_d = 0.017, Re_d = 5.4, We_d = 0.088 for the perpendicular inlet flow configuration.

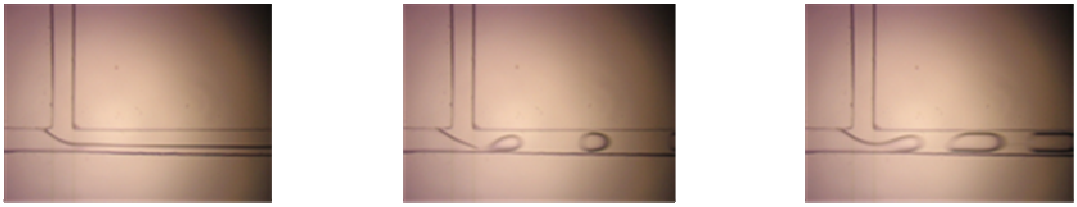

Figure 11: Cycles between (a) stable parallel flow, (b) droplet and (d) plug formation at Qc = 25µl/min, Q =1, Ca_c = 0.48, Re_c = 0.16, Ca_d = 0.017, Re_d = 5.4, We_d = 0.088 for the horizontal inlet flow configuration.

Table 3: Results of the flow behaviour observed under different fluid inlet geometries

Flow conditions	Perpendicular	Horizontal	Symmetrical
Q_c = 5µl/min, Q = 3, Ca_c = 0.1, Re_c = 0.031, Ca_d = 0.0099, Re_d = 3.2, We_d = 0.032	Instability cycles	Instability cycles	Instability cycles
Q_c = 5µl/min, Q = 5, Ca_c = 0.1, Re_c = 0.031, Ca_d = 0.017, Re_d = 5.4, We_d = 0.088	Instability cycles	Instability cycles	(Convectively) unstable stratified
Q_c = 5µl/min, Q = 8, Ca_c = 0.1, Re_c = 0.031, Ca_d = 0.026 Re_d = 8.6, We_d = 0.23	(Convectively) unstable stratified	(Convectively) unstable stratified	(Convectively) unstable stratified
Q_c = 5µl/min, Q = 16, Ca_c = 0.1, Re_c = 0.031, Ca_d = 0.053 Re_d = 17.1, We_d = 0.9	Parallel	Parallel	Parallel
Q_c = 25µl/min, Q = 1, Ca_c = 0.48, Re_c = 0.16, Ca_d = 0.017, Re_d = 5.4, We_d = 0.088	Instability cycles	Instability cycles	Plugs
Q_c = 25µl/min, Q = 2, Ca_c = 0.48, Re_c = 0.16, Ca_d = 0.033, Re_d = 10.7, We_d = 0.35	Parallel	Parallel	Parallel

5 Conclusions and Recommendations for Future Work

We have, through experiments, observed in a microfludic T-junction the existence of flow regimes where convective instability co-exists interchangeably with the absolute instability, as a function of time. We conclude that the instabilities are the result of interplay between interfacial, viscous and inertial forces. Existence of parallel flow is attributed to dominance of inertial effects of the water phase. It is envisaged that different fluid interfacial tensions and viscosity ratio will be investigated to increase the scope of this study. There is very little influence of fluid inlet geometry on the behaviour of the instabilities. Deviations were observed on the symmetrical inlet configurations. Linear stability analysis will be conducted to gain further insight into the cycles of instabilities as a tempo-spatial function.

References

1. A. Huebner, S. Sharma, M. Srisa-Art, F. Hollfelder, J.B. Edel, A.J. Demello. *Lab Chip;* 8(8), 1244-54 (2008).
2. D.L. Chen, L. Li, S. Reyes, D.N. Adamson, and R.F. Ismagilov, *Langmuir 23,* 2255-2260 (2007).
3. J. Plateau, Gauthier-Villars, Paris, (1873).
4. L. Rayleigh, *Proc. London Math. Soc. 10*, 4 (1878).
5. L. Rayleigh, *Philos. Mag. 34*, 145 (1892).
6. P. Guillot, A. Ajdari, J. Goyon, M. Joanicot, A. Colin, *C. R. Chimie,* (2009),12, 247-257
7. K.J. Humphry, A. Adjari, A. Fernandez-Nieves, H.A. Stone, D.A. Weitz, *Phys. Rev. E. 79*, 056310 (2009).
8. M.A. Herrada, A.M. Ganan-Calvo, P. Guillot *Phys. Rev. E. 78,* 046312 (2008).
9. P. Guillot, A. Colin, A.S. Utada, A. Adjari, *Phys. Rev. Lett. 99,* 104502 (2007)
10. P. Guillot et al *Langmuir 22,* 6438-6445 (2006).
11. P. Guillot, A Colin, *Phys. Rev. E. 72,* 066301 (2005).
12. A.S. Utada, A. Fernandez-Nieves, H.A. Stone, D.A. Weitz, Dripping to jetting transitions in co-flowing liquids, *Phys. Rev. Lett.* 99, 094502 (2007).
13. A.S. Utada, A. Fernandez-Nieves, J.M. Gordillo, D.A. Weitz, *Phys. Rev. Lett.* 100, 014502 (2008)
14. J.H. Xu, S.W. Li, J. Tan, Y.J. Wang, G.S. Luo, *AIChE J. 52*, 9, 3005–3010 (2006)
15. P. Garstecki, M.J. Fuerstman, H.A. Stone, G.M. Whitesides, *Lab Chip 6*,437–446 (2006)
16. J.H. Xu, S.W. Li, J. Tan, Y.J. Wang, G.S. Luo, Microfluid. Nanofluid. 5,711-717 (2008)
17. H.A. Stone, *J. Fluid. Mech. 595*, 141–161(2008).
18. Tabeling P (2005) Introduction to microfluidics. P45, Oxford University press, Oxford.
19. Bruus H (2008) Theoretical Microfluidics, p2, Oxford University press, Oxford.